TISSUE ENGINEERING: Part A
Volume 16, Number 8, 2010

DOI: 10.1089/ten.tea.2009.0815

Microtopographical Cues in 3D Attenuate Fibrotic Phenotype and Extracellular Matrix Deposition: Implications for Tissue Regeneration

Perla Ayala, B.S.,[1,2] Jose I. Lopez, Ph.D.,[3] and Tejal A. Desai, Ph.D.[1,2,4]

Recent studies have highlighted the role of external biophysical cues on cell morphology and function. In particular, substrate geometry and rigidity in two dimensions has been shown to impact cell growth, death, differentiation, and motility. Knowledge of how these physical cues affect cell function in three dimensions is critical for successful development of novel regenerative therapies. In this work, the effect of discrete micromechanical cues in three-dimensional (3D) system on cell proliferation, gene expression, and extracellular matrix synthesis was investigated. Poly(ethylene glycol) dimethacrylate hydrogel microrods were fabricated using photolithography and suspended in gel to create a 3D culture with microscale cues of defined mechanical properties in the physiological range (2–50 kPa). These microrods significantly affected fibroblast proliferation, matrix production, and gene expression. Cultures with stiff microrods reduced fibroblast proliferation and downregulated expression of key extracellular matrix proteins involved in scar tissue formation. In addition, the contractility marker alpha smooth muscle actin and adhesion molecule integrin α3 were also significantly downregulated. Cultures with soft microrods had no significant difference on fibroblast proliferation and expression of Cyclin D1, alpha smooth muscle actin, and integrin α3 compared to cultures with no microrods. Here, we present a new platform of potentially injectable microrods with tunable elasticity; in addition, we show that cell proliferation and gene expression are influenced by discrete physical cues in 3D.

Introduction

There is increasing evidence that the efficacy of tissue regeneration is likely dependent on creating a suitable microenvironment that can support cell function and decrease pathological healing. For example, recent findings have demonstrated that the functional improvements associated with the direct delivery of hematopoietic stem cells to the heart are not due to their capacity to differentiate into myocytes, but rather due to their secretion of factors that appear to be beneficial for angiogenesis.[1–3] One issue regarding cell retention or death may be caused by defects of the microenvironment. An environment is needed that allows for perfect, rather than suboptimal, healing, one in which the type and amount of extracellular matrix (ECM) synthesis is suitable for the tissue regeneration, rather than fibrous scarring. In the last several years, mechanical, topographical, and geometrical cues have been shown to modulate cellular morphology and behavior in two-dimensional (2D) and three-dimensional (3D) systems.[4–12] However, the potential to control fibroblast behavior and ECM synthesis using discrete microtopographical cues has not been fully explored. This knowledge could provide a better understanding of the role of topography in matrix remodeling, with the potential to enhance regenerative therapies. *In vivo*, the intrinsic chemical and mechanical properties of the ECM play a critical role in controlling the organization, proliferation, differentiation, and migration of stem[13,14] and mature[15–18] cell populations. In particular, numerous studies have shown that the rigidity of the ECM can have a significant effect on cellular phenotype, migration, and differentiation.[7,19,20] Mesenchymal stem cells (MSCs) differentiate to a specific lineage depending on the elasticity of the matrix in 2D[7] and fibroblasts preferentially proliferate in 3D rigid gels and migrate more in flexible ones.[21] Further, an increase of rigidity in the matrix could also be associated with pathological conditions such as cancer and heart failure.[22,23]

[1]Joint Graduate Group in Bioengineering, University of California San Francisco–University of California Berkeley, San Francisco, California.
Departments of [2]Bioengineering and Therapeutic Sciences, [3]Surgery, and [4]Physiology, University of California, San Francisco, California.

Stiffening of tissue can be directly attributed to fibrosis, the over deposition of ECM proteins. Chronic forms of fibrotic diseases cause almost 45% of all deaths in the developed world.[24] Pathological production of ECM has been well recognized in the heart, liver, lung, kidney, bone marrow, cornea, spinal cord, skin, and even in the tumor stroma microenvironment.[22,24–28] A particular case where fibrosis prevents tissue regeneration can be observed in the myocardium after a heart attack. Studies have found an increase in collagen I, collagen III, and collagen VI production in cardiac pathology after myocardial infarction.[29–31] Fibrous tissue appears in the infarcted and also noninfarcted myocardium.[29] The measured elastic modulus of myocardium in healthy rats yields $E = 18$ kPa, whereas there is a threefold increase ($E = 60$ kPa) for infarcted myocardium.[32] Tissue stiffness has been shown to have a critical effect on cardiomyocyte function with scar-tissue rigidity having an adverse effect on embryonic cardiomyocyte beating. Injected MSCs have been shown to reduce the stiffness of scar formation after myocardial infarction,[32] whereas another study showed that injection of MSCs resulted in the generation of ossifications in the infarcted myocardium.[33]

Fibroblasts are the main synthesizers of ECM, but after injury they acquire a contractile phenotype characterized by the expression of alpha smooth muscle actin (α-*SMA*).[34] Interstitial fibroblasts are responsible for collagen synthesis in the normal myocardium, whereas contractile fibroblasts, termed "myofibroblasts," have been associated with fibrosis at the site of injury after a myocardial infarction.

Controlling fibroblast numbers and aberrant collagen production is a critical step to sustain the intrinsic tissue regeneration process. By manipulating the cues that cells encounter in the microenvironment, it may be possible to guide cell behavior and support tissue regeneration. Previously, we have shown that microtopography plays an important role in fibroblast proliferation. Micropegs on a 2D surface decrease proliferation of fibroblasts compared to flat surfaces.[4] In addition, this was correlated with a significant decrease in Cyclin D1 expression, demonstrating that cell proliferation was affected at the level of G1/S cell cycle transition.[4] Further, this effect was dependent on local micropeg–cell interactions and was regulated by contractile mechanics.[35] Subsequently, we showed that microtopographical cues in a 3D system also inhibit fibroblast proliferation. SU-8 epoxy microrods suspended in Matrigel significantly inhibited the proliferation of the fibroblasts compared to a 3D Matrigel culture without microrods.[10] Recently, we have also shown that these stiff epoxy microrods could have an opposite effect on stem cells in a 3D culture. These same microstructures increased human MSC proliferation and slowed osteogenic differentiation.[36]

Although there are some studies that have addressed the effect of mechanical stretching on fibroblast phenotype and ECM synthesis,[37–40] little is known about the combined effect of substrate stiffness and microtopography on fibroblasts and ECM synthesis. Effective strategies to avert the development of fibrosis while allowing overall repair would represent a critical therapeutic innovation.[41] In this work, we develop a biocompatible microrod system with tunable mechanical properties to investigate the role of 3D micromechanical cues on fibroblast function.

Materials and Methods

Poly(ethylene glycol) dimethacrylate microrod fabrication

Microrods were fabricated using a precursor solution consisting of poly(ethylene glycol) dimethacrylate (PEGDMA) MW 750 (Sigma-Aldrich), photo-initiator 2,2-dimethoxy-2-phenylacetophenone (Sigma-Aldrich) dissolved in 1-vinyl-*n*-pyrrolidone (Sigma-Aldrich) crosslinker (100 mg/mL), and 1× phosphate-buffered saline (PBS). Microrods were created with different magnitudes of stiffness by varying the PEGDMA (90%, 50%, and 10% w/v) and the photoinitiator-crosslinker concentrations (0.8%, 0.1%, and 0.04% w/v). The hydrogel precursor solution was sonicated at room temperature (VWR Model 75T; West Chester) for 15 min to ensure complete mixing of reagents.

Photolithography was used to create microrods designed to be 100 μm long with a 15×15 μm cross section. Microrods were micro-fabricated in 3-inch silicon wafers. Each wafer was cleaned in piranha solution (3:1; H_2SO_4:H_2O_2) for 20 min, and rinsed with deionized water three times. Wafers were then rinsed with acetone, methanol, and isopropanol, and then baked at 200°C for 2 min. The PEGDMA precursor solution was then spun onto each wafer to achieve a desired thickness of 15 μm. The wafer was exposed using a Karl Suss MJB3 mask aligner to a 405 nm light source through the microrod patterned photomask at 9 mW/cm^2 until crosslinking. The height of the microstructures was confirmed using an Ambios Technology XP-2 profilometer (Fig. 2). Microrods on the wafer were then rinsed with isopropanol and dried with N_2 gas. Microrods were removed from the wafer by rinsing wafer with 70% ethanol and gently scraping microrods with a cell scraper. Collected microrods were centrifuged and rinsed in 70% ethanol three times. Microrods were then centrifuged and rinsed with sterile 1× PBS three times. Microrods were finally resuspended in the cell culture medium.

Cell culture

NIH 3T3 mouse fibroblasts were cultured in the complete medium consisting of Dulbecco's modified Eagle's medium with 10% fetal bovine serum and 1% penicillin/streptomycin (Gibco-BRL). Cell cultures were maintained in a humidity-controlled 5% CO_2 incubator at 37°C and were allowed to grow to ~90% confluence. Before seeding, cells were trypsinized and resuspended in the complete medium. For 2D cultures, the microrods remained attached to the surface, and cells were plated at a density of 10,000 cells/cm^2 and washed after 1 h to remove nonadherent cells. Cultures were fixed after 5 days. For 3D cultures, cells were initially seeded at a concentration of 2500 cells per 65 μL of low growth factor Matrigel (BD Biosciences) (4 mg/mL) either without microrods or with microrods at a seeding ratio of 1:5 number of microrods to number of cells into individual wells in a 96-well plate. This resulted in 2-mm-thick gels. The plate was incubated at 37°C for 30 min to allow gels to solidify completely. Each gel was then covered with 200 μL of the medium, and the plate was placed in an incubator at 37°C for 5 days.

Fluorescent microscopy

Cells were fixed in 4% paraformaldehyde (Fisher Scientific) for 15 min, permeabilized with 0.5% Triton X-100 (Sigma) for 15 min, and blocked with 1% bovine serum albumin (Sigma) for 30 min. F-actin was stained using Alexa Fluor 488 phalloidin (Molecular Probes) for 30 min. Nuclei were then stained with Hoechst 33258 (Molecular Probes) for 5 min. The Hoechst solution and the Alexa Fluor were also absorbed by the PEGDMA microrods, allowing us to easily observe the rods in 3D culture. Images were acquired using an Olympus BX 60 microscope, a Nikon TE2000E motorized inverted microscope, or a Nikon C1si spectral confocal.

Scanning electron microscopy

Samples were dehydrated by adding and replacing a series of ethanol solutions in a graded series (35%, 50%, 70%, 95%, and 100%). The final 100% ethanol solution was replaced with hexamethyldisilazane (PolySciences, Inc.) for 10 min and removed rapidly. Samples were allowed to dry completely in vacuum overnight and analyzed in a Novelx *my*SEM.

Proliferation assay

Cellular proliferation was assessed at 5 days after initial seeding in the gels using a 3-(4,5-dimethylthiazol-2-yl)-2,5-diphenyltetrazolium bromide (MTT) assay (Sigma-Aldrich). On the day of the assay, the medium was removed from the wells and was replaced with 100 μL of the fresh growth medium and 16.5 μL of the MTT reagent. The plate was then placed back in the incubator for 4 h. Then, the formazan crystals were dissolved with the solubilization solution, and the absorbance was measured and compared to a standard curve to calculate the number of cells present.

Stiffness characterization

Films of various PEGDMA concentrations (90%, 50%, and 10% w/v) and photoinitiator-crosslinker concentrations (0.8%, 0.1%, and 0.04% w/v) were prepared for stiffness characterization. For each hydrogel film, 100 μL of the precursor solution was placed on a glass slide. The glass slide was exposed using a Karl Suss MJB3 mask aligner to a 405 nm light source at 9 mW/cm^2 until crosslinking. The hydrogels were rinsed once with 1× PBS and then soaked in 1× PBS for 1 week. Hydrated films of various PEGDMA and crosslinker concentrations were attached on a glass slide and mounted onto the stage of an Asylum MFP-3D atomic force microscope (Asylum Research) coupled to a Nikon TE2000U epifluorescence microscope. Force measurements were obtained using Olympus silicon nitride cantilevers with nominal spring constants of 2.0 N/m. Measurements were done on 1× PBS wetted film surface. Displacement versus position data were converted to force versus indentation based on the estimated hard contact position, which was fitted to a Hertzian model to obtain Young's moduli. Force loading was applied to at least three sites in each sample.

RNA isolation and reverse transcription

Total RNA was isolated from fibroblasts 5 days after culture. Trizol (Invitrogen) and Qiagen microRNA purification columns were used to isolate and purify RNA according to the manufacturer's protocol. Genomic DNA contamination was removed by treating the isolated RNA using RQ1 RNase-Free DNase (Promega). RNA concentrations were quantified using a NanoDrop spectrophotometer (Thermo Scientific). RNA was reverse transcribed using iScript cDNA (BioRad) and a thermal cycler Mastercycler S (Eppendorf) according to the manufacturer's protocol (5 min at 25°C, 30 min at 42°C, and 5 min at 4°C).

Quantitative polymerase chain reaction

Quantitative polymerase chain reaction (q-PCR) was performed with Power SYBR Green PCR Master Mix and a StepOne Plus Real-Time PCR System (Applied Biosystems). To ensure specificity of PCR, melt–curve analyses were performed at the end of all PCRs. The relative amount of target cDNA was determined from the appropriate standard curve and normalized by the amount of glyceraldehyde 3-phosphatedehydrogenase (*GAPDH*) cDNA present in each sample. Primers (Integrated DNA Technologies) are provided in Table 1. Each sample was analyzed in triplicate, and results were expressed relative to *GAPDH* as an endogenous control.

Contractility inhibition studies

To investigate the impact of cellular contractility, (Y-27632; Calbiochem) was used to inhibit Rho-associated kinase (ROCK) and (ML-7; Calbiochem) was used to inhibit myosin light chain kinase (MLCK). Both drugs were diluted to 25 μM in the complete medium before addition to the cultures. In all cases, cells were seeded and allowed to attach and spread for 1 h before application of the drug, and the drug was left in the culture for 5 days before analysis. For contractility inhibition studies, messenger RNA levels were quantified using a Fast SYBR® Green Cells-to-CT™ Kit (Applied Biosystems). Reverse transcription was performed on a Mastercycler S (Eppendorf). qPCR was performed using a StepOne Plus (Applied Biosystems). Each sample was analyzed in triplicate, and results were expressed relative to *GAPDH* as an endogenous control.

Table 1. Quantitative Polymerase Chain Reaction Primers

Gene	*Primer sequence (5′–3′)*
GAPDH	F: TGGCCTCCAAGGAGTAAGAAAC
Col I	R: GGGATAGGGCCTCTCTTGCT
	F: GCACGAGTCACACCGGAACT
	R: AAGGGAGCCACATCGATGAT
Col VI	F: ACCCGGGACCGGCTACT
	R: CAGAACGTCCATCCGTAATGAC
α-SMA	F: TCCTGACGCTGAAGTATCCGATA
	R: GGTGCCAGATCTTTTCCATGTC
INT α3	F: ATCATCCTCCTCTTGTGGAAGTG
	R: GCCTTCTGCCTCTTAGCTTCATA
Cyclin D1	F: AGCCAGCTGCAGTGCTGTAG
	R: CTGGTGGTGCCCGTTTTG

Col I, collagen type I; *Col VI*, collagen type VI; *GAPDH*, glyceraldehyde 3-phosphatedehydrogenase; *INT α3*, integrin α3; *α-SMA*, alpha smooth muscle actin.

Statistical analysis

A statistically significant difference among groups was detected by analysis of variance. Sequential Holm *t*-tests were then performed to identify differences between specific pairs of conditions.

Results

In this work, the mechanical properties of PEGDMA hydrogels were altered by both varying the monomer concentration while maintaining a set crosslinker concentration and changing crosslinker concentration while keeping monomer concentration constant. The elastic moduli of PEGDMA hydrogel films of various monomer and crosslinker concentrations were analyzed by atomic force microscopy (Fig. 1). For the hydrogels analyzed in these studies, changing the crosslinker concentration in PEGDMA hydrogels yielded greater elastic modulus range (2–50 kPa) than varying the monomer concentration (1.5–20 kPa).

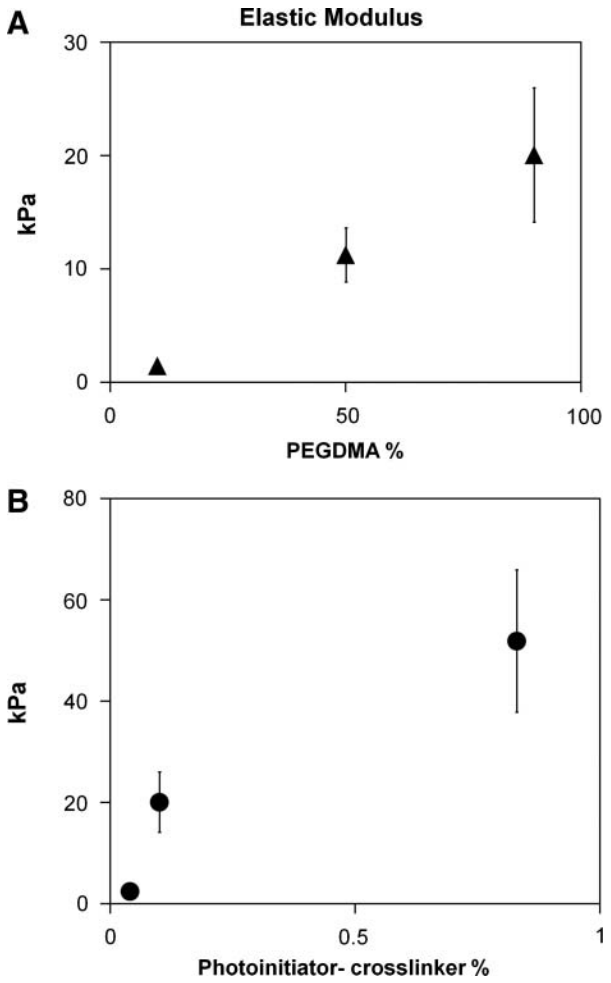

FIG. 1. The elastic modulus of PEGDMA hydrogels can be controlled by varying the monomer and crosslinker concentration. (**A**) PEGDMA concentration was varied from 10% to 90%, with photoinitiator-crosslinker concentration at 0.1%. (**B**) Photoinitiator-crosslinker was varied from 0.04% to 0.8% (w/v), with PEGDMA concentration constant at 90%. Bars indicate SD. PEGDMA, poly(ethylene glycol) dimethacrylate; SD, standard deviation.

Photolithography was used to create microrods of $H = 15$ μm, $W = 15$ μm, and $L = 100$ μm with physiological stiffness[19] (2–50 kPa) by varying crosslinker concentration while keeping the monomer concentration constant (Fig. 2). This allowed for the development of microrods with very similar chemical composition but different mechanical properties in the physiological stiffness range. The length and width of the microrods are controlled by the mask, whereas the height of the microrod is controlled by the spin rate. By maintaining the monomer concentration, the viscosity of the precursor solution was unchanged allowing the spin rate to be consistent, thus enabling the fabrication of reproducible sized microrods with a range of elastic moduli.

To ensure that microrods were not toxic and to examine the interaction of fibroblasts with these hydrogel microstructures, fibroblasts were cultured on 2D surfaces with attached PEGDMA microrods (100×100 μm spacing). We observed that cells closely interacted with microrods of all stiffness in 2D. Interestingly, they formed a distinct ordered architecture when in contact with the microrods even when not functionalized with adhesive ligands. Cells not only grow in the presence of the microrods but are able to attach, align, and organize their cytoskeleton with the microrod topography (Fig. 3).

For 3D studies, cells were seeded within Matrigel scaffolds, a solubilized basement membrane rich in ECM proteins that mimic a natural ECM environment.[42,43] To elucidate the impact of micromechanical and topographical cues on cell proliferation within a 3D microenvironment, 3T3 fibroblasts were cultured in Matrigel with PEGDMA microrods of different stiffness (2, 20, and 50 kPa) at an initial microrod to cell ratio of 1:5 in a 3D Matrigel gel for 5 days. This range of microrod stiffness was investigated since it is physiological relevant to both, a healthy myocardium (18 kPa) and an infarcted myocardium (>50 kPa).[32] Fluorescent microscopy shows that 3T3 fibroblasts cultured with microrods in a 3D Matrigel directly interact and stretch along and across microrods (Fig. 4) in a similar manner as seen in 2D cultures (both aligning and bridging with microrods). An MTT assay was used to assess proliferation of fibroblasts in Matrigel gels. An absorption standard curve was determined for fibroblasts growing in 3D Matrigel. This allowed for the determination of the linear range of absorption for experimental cell concentrations. The inclusion of microrods at the concentrations used did not cause changes in the absorbance. Therefore, changes in absorbance were only attributed to differences in cell number. In addition, we had previously shown that the incorporation of stiff microrods in the composite Matrigel did not change its mechanical properties compared to Matrigel without microrods.[10] Our data show that gels with stiffer microrods (20 and 50 kPa) significantly downregulated fibroblast proliferation compared to gels with no microrods (Fig. 5). Soft microrods (2 kPa) appear to have a lesser effect (not statistically different) on fibroblast proliferation. The greatest effect in cell number was observed with the 20 kPa microrods. The percent cell number difference after 5 days in culture between the gels with no microrods and gels with microrods was 29%, 34%, and 23% for 50, 20, and 2 kPa microrods, respectively.

We also investigated whether local microscale domains could cause alterations in Cyclin D1, an important regulator of the G/S cell cycle transition, and in collagen type I (*Col I*)

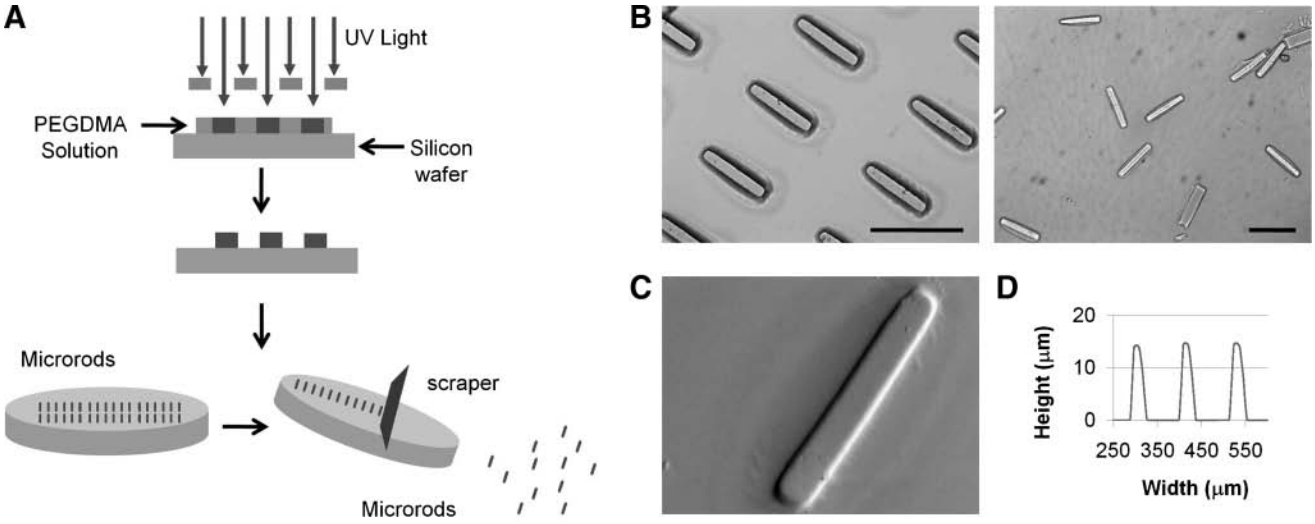

FIG. 2. (**A**) Schematic of PEGDMA microscaffold fabrication by photolithography. (**B**) Bright-field images of microrods attached and microrods released from substrate. (**C**) Scanning electron microscopy image of PEGDMA microrods. (**D**) Profile graph of microrods. Scale bars: 100 μm.

and collagen type VI (*Col VI*) expression. Expression of α-*SMA* and integrin α3, two cell markers that are also elevated postmyocardial infarction,[31] was also investigated. Expression of these genes was analyzed by qPCR. In our study *Col I* and *Col VI* were downregulated in cell populations cultured with all three stiffness microrods, suggesting that microstructures can be used to modulate ECM synthesis. Not only was collagen downregulated in all three microrod cultures, but also microstructure stiffness has profound effects on other fibrotic cell markers (Fig. 6). Cultures with soft microrods showed no significant difference on expression of Cyclin D1, α-*SMA*, and integrin α3 compared to cultures with no microrods. However, fibroblasts seeded with stiffer microrods (20 and 50 kPa) showed downregulation of Cyclin D1, the contractility marker α-*SMA*, and integrin alpha 3 with the most pronounced effect being observed in the 20 kPa microrod system (Fig. 6). This response to the stiffer microstructures suggests that a reduction in cell proliferation may be associated with an alteration in mechanotransduction; cells attached to stiffer microrods generate a mechanical force that results in changes in cell proliferation.

To investigate if downregulation of collagen by the microrods was dependent on the cells' ability to sense the microrods through changes in contractiltity, we pharmacologically inhibited both ROCK and MLCK in cells grown in gels without microrods and in gels with 50 kPa microrods. Direct phosphorylation of MLC by ROCK leads to contractile force generation. Independent from RhoA, phosphorylation of MLC can also be regulated by MLCK. When cultured in the presence of ROCK inhibitor Y27632, or MLCK inhibitor ML7, fibroblasts showed no change in *Col I* expression in the presence of microrods compared to gels with no microrods (Fig. 7).

Discussion

Previous studies on substrate stiffness and microtopography have been done utilizing polyacrylamide, polydimethylsiloxane, and SU-8 (epoxy polymer) substrates among others.[4,5,7,10,11] Although these materials are useful for *in vitro* experiments, they do not offer the necessary biocompatibility and mechanical/geometrical tunability for

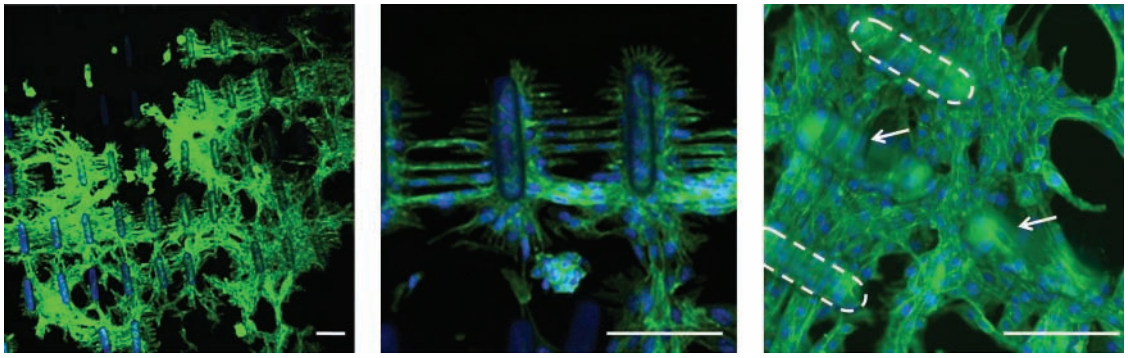

FIG. 3. Fibroblasts on two-dimensional surface bridge and align with PEGDMA microrods (50 kPa). F-actin (Alexa fluor 488), and cell nuclei (Hoechst). Arrow and dashed lines indicate microrods. Scale bars: 100 μm. Color images available online at www.liebertonline.com/ten.

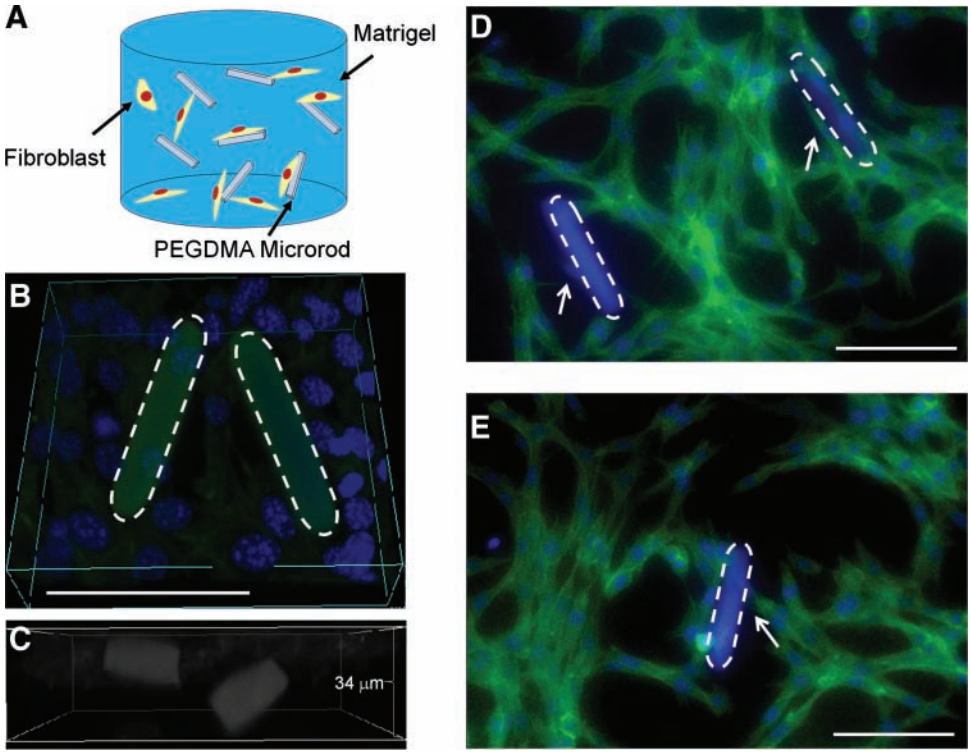

FIG. 4. (**A**) Schematic of 3D system. Fibroblasts and microrods encapsulated within Matrigel. (**B**) 3D Reconstruction of fibroblasts and PEGDMA microrods in Matrigel. (**C**) Microrods in different z-planes within the gel. (**D, E**) Fibroblasts attach and link PEGDMA microrods (50 kPa) in 3D cultures. F-actin (Alexa fluor 488), cell nuclei (Hoechst). Dashed lines indicate microrods. Arrows indicate cells attaching to microrods. Scale bars: 100 μm. 3D, three-dimensional. Color images available online at www.liebertonline.com/ten.

therapeutic purposes. In this study, PEGDMA was utilized because it can be crosslinked in the presence of UV light, allowing for the size and geometry to be easily controlled by photolithography. In addition, the mechanical properties of PEG acrylates can be tuned by varying PEG molecular weight, monomer concentration, and crosslinking density.[12,44,45]

Previous studies have also focused on the effects of 2D substrate stiffness or 3D homogeneous matrix properties.[46–48] In contrast, this PEGDMA microrods system was developed to investigate the effect of micromechanical domains on cell proliferation and gene expression in 3D. Fibroblasts were cultured in Matrigel with microrods of different stiffness (2, 20, and 50 kPa). These microrods attenuate the production of collagen from fibroblasts and the cells respond most dramatically to cues that have muscle-like stiffness values. The effect of these micromechanical domains on cell behavior is striking considering that the microrod structures account for only 0.017% of the total 3D matrix. Expression of α-*SMA* in fibroblasts has been shown to be influenced by the mechanical microenvironment and the organization and the rigidity of the ECM.[34] In addition, studies have shown that mechanical stretching can influence collagen production.[37,39,49] In our studies, both collagen and α-*SMA* were regulated by the micromechanical domains in 3D culture.

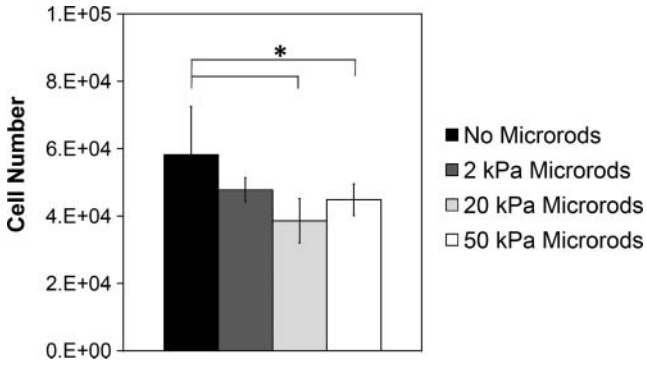

FIG. 5. Fibroblast proliferation was significantly reduced in gels with microrods of higher stiffness (20 and 50 kPa), but no significant difference was found with softer microrods (2 kPa) as analyzed by MTT assay. Bars indicate SD and asterisk (*) indicates $p < 0.05$ ($n = 6$).

Although many collagen types are expressed in the myocardium, collagen type plays a significant role on cell behavior.[50–52] In particular, *Col VI* plays a critical role in the origin of fibrosis in the heart and other diseased tissues.[27,52–54] Interestingly, in our studies expression of *Col IV* correlates with that of α-*SMA*, and integrin α3 in the different culture conditions. This association is in agreement with previous observations on myofibroblast studies, where it has been shown that *Col VI* induces the cardiac myofibroblast phenotype[52] and that *Col VI* interacts with the α3 integrin receptor in fibroblasts.[31] Blockade of the α3 integrin receptor has been correlated to an attenuation of *Col VI*–induced myofibroblast differentiation.[31] A recent study has also shown that deletion of integrin α3 prevented epithelial–mesenchymal transition, a source of myofibroblasts in lung fibrosis.[55] These results also implicate integrin α3 as an important regulator of cell phenotype and matrix deposition. Our studies show that expression of this molecule could be downregulated by stiffer microrods with greatest effect observed when fibroblasts where seeded amongst 20 kPa microrods. Soft microrods (2 kPa) do not significantly downregulate Cyclin D1, α-*SMA*, or integrin α3. We speculate that microrods of muscle-like stiffness (~20 kPa) direct fibroblasts to behave more like

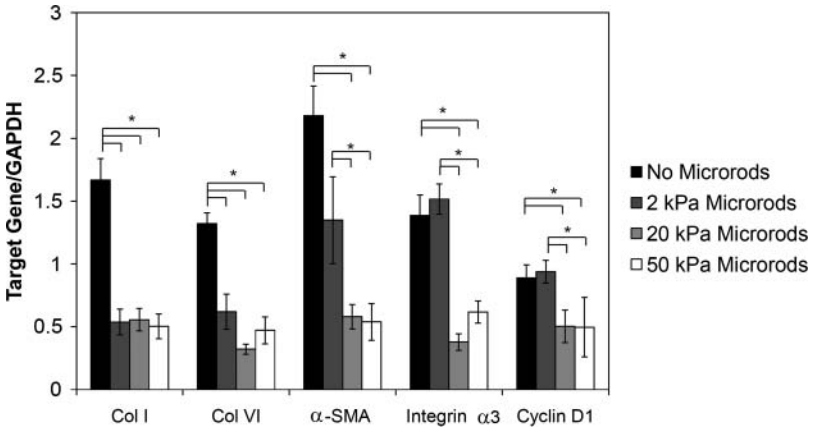

FIG. 6. PEGDMA microrods of different stiffness have a varied response on extracellular matrix synthesis and gene expression in 3D gels. Collagens I and VI were downregulated in all microrod cultures. Fibroblasts with stiffer microrods showed downregulation of Cyclin D1, contractility marker α-*SMA*, and integrin α3. Cultures with soft microrods showed no significant difference on expression of Cyclin D1, α-*SMA*, and integrin α3 compared to cultures with no microrods. Bars indicate SD and asterisks (*) indicate $p < 0.05$ ($n = 6$). *Col I*, collagen I; *Col VI*, collagen VI; α-*SMA*, alpha smooth muscle actin.

interstitial fibroblasts, whereas softer microrods seem to direct cells to more myofibroblastic behavior.

Interestingly, when fibroblasts' myosin-based contractility was inhibited by two different independent mechanisms (ROCK and MLCK), there was no downregulation of collagen synthesis, suggesting that the actual interaction with the microrod and subsequent changes in contractility are responsible for the differences in collagen synthesis. This is consistent with previous observations in 2D micropeg surfaces where modulation of cell proliferation was found to be contractility dependent.[35]

In vivo, lack of matrix support could be associated with initial collagen deposition as seen in the first days after myocardial infarction, with stiffer matrix formation occurring after long-term fibrosis. This correlates with the presence of myofibroblasts and *Col VI* after myocardial infarction, where there is an elevation within the first week with reduced expression after 2 weeks, but persist after 20 weeks.[31,52] Myocardial regeneration requires migration and growth of cardiac progenitors and myocytes in the infarct area, a system capable of maintaining low fibroblasts, while promoting muscle regeneration will be a critical step toward this goal. Our data suggest that microrods could provide structural support that prevents fibroblasts from acquiring a more fibrotic state, therefore limiting deposition of matrix molecules.

This study demonstrates the ability of discrete topographical cues to affect cell proliferation, gene expression, and matrix production in a 3D system. To our knowledge, this is the first study that investigates the effect of discrete microscale cues of different stiffness on cell function in 3D. The results from these studies have promising implications not only for tissue-engineered constructs but also for stem cell studies in 3D systems *in vitro* and *in vivo*.

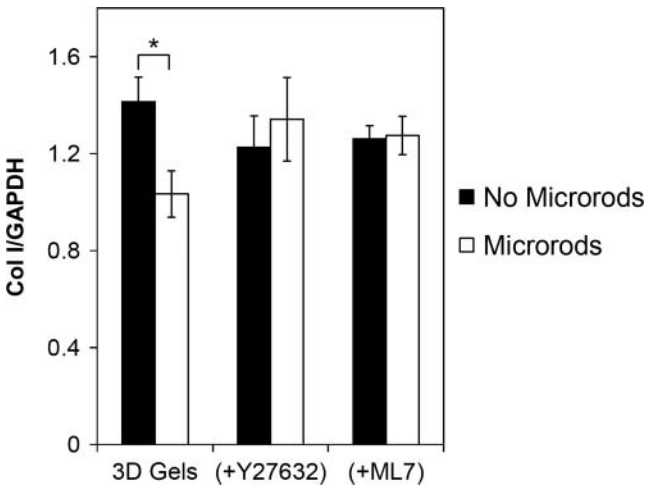

FIG. 7. Fibroblasts cultured in the presence of Rho-associated kinase inhibitor Y27632, or myosin light chain kinase inhibitor ML7, showed no change in *Col I* expression in the presence of microrods (50 kPa) compared to gels with no microrods. Bars indicate SD and asterisk (*) indicates $p < 0.05$ ($n = 3$).

Conclusions

We fabricated a new microrod scaffold system from PEGDMA that is biocompatible, mechanically tunable, and compatible with photolithographic processing. We created a scaffold system consisting of polymeric microrods of different stiffness embedded in a 3D matrix to investigate the role of discrete micromechanical cues on cell proliferation, gene expression, and ECM synthesis. Microrods that were seeded with fibroblasts in a 3D biopolymer matrix affected cell behavior in terms of proliferation and gene expression. Stiffer microrods reduce fibroblast proliferation, collagen deposition, and fibrotic phenotype expression, whereas softer microrods showed no significant effect. These microstructures offer numerous possibilities for *in vitro* studies involving the effect of discrete mechanical cues on stem cells, progenitor cells, or even terminal cells such as myocytes in 3D cultures. The microrods can potentially also be used as injectable microscaffolds to influence tissue regeneration *in vivo*.

Acknowledgments

The authors appreciate Dr. Kurt Thorn's training and assistance at the Nikon Imaging Center at UCSF–Mission Bay. In addition, the authors thank Dr. Dan Han and Lily Peng for their guidance in RNA isolation and qPCR; Dr. Daniel A. Bernards and Kayte Fischer for facilitating scanning electron microscopy training; and Dr. Kristy Ainslie, Dr. Rahul Thakar, Dr. Rachel Lowe, and Dr. Miquella Chavez for insight and advice. The authors also thank the UCSF Biomedical Micro- and Nanofabrication Core for

allowing them to fabricate their PEGDMA microstructures. This research was partially supported by the National Science Foundation (NSEC), National Institutes of Health, a National Science Foundation Graduate Fellowship to P.A., and a University of California, Berkeley Chancellor's Fellowship to P.A.

Disclosure Statement

No competing financial interests exist.

References

1. Fazel, S., Cimini, M., Chen, L., Li, S., Angoulvant, D., Fedak, P., Verma, S., Weisel, R.D., Keating, A., and Li, R.K. Cardioprotective c-kit+ cells are from the bone marrow and regulate the myocardial balance of angiogenic cytokines. J Clin Invest **116,** 1865, 2006.
2. Paul, D., Samuel, S.M., and Maulik, N. Mesenchymal stem cell: present challenges and prospective cellular cardiomyoplasty approaches for myocardial regeneration. Antioxid Redox Signal **11,** 1841, 2009.
3. Kawamoto, A., Iwasaki, H., Kusano, K., Murayama, T., Oyamada, A., Silver, M., Hulbert, C., Gavin, M., Hanley, A., Ma, H., Kearney, M., Zak, V., Asahara, T., and Losordo, D.W. CD34-positive cells exhibit increased potency and safety for therapeutic neovascularization after myocardial infarction compared with total mononuclear cells. Circulation **114,** 2163, 2006.
4. Boateng, S.Y., Hartman, T.J., Ahluwalia, N., Vidula, H., Desai, T.A., and Russell, B. Inhibition of fibroblast proliferation in cardiac myocyte cultures by surface microtopography. Am J Physiol Cell Physiol **285,** C171, 2003.
5. Brown, X.Q., Ookawa, K., and Wong, J.Y. Evaluation of polydimethylsiloxane scaffolds with physiologically-relevant elastic moduli: interplay of substrate mechanics and surface chemistry effects on vascular smooth muscle cell response. Biomaterials **26,** 3123, 2005.
6. Chen, C.S., Mrksich, M., Huang, S., Whitesides, G.M., and Ingber, D.E. Geometric control of cell life and death. Science **276,** 1425, 1997.
7. Engler, A.J., Sen, S., Sweeney, H.L., and Discher, D.E. Matrix elasticity directs stem cell lineage specification. Cell **126,** 677, 2006.
8. Kim, D.H., Kim, P., Song, I., Cha, J.M., Lee, S.H., Kim, B., and Suh, K.Y. Guided three-dimensional growth of functional cardiomyocytes on polyethylene glycol nanostructures. Langmuir **22,** 5419, 2006.
9. Nelson, C.M., Jean, R.P., Tan, J.L., Liu, W.F., Sniadecki, N.J., Spector, A.A., and Chen, C.S. Emergent patterns of growth controlled by multicellular form and mechanics. Proc Natl Acad Sci U S A **102,** 11594, 2005.
10. Norman, J.J., Collins, J.M., Sharma, S., Russell, B., and Desai, T.A. Microstructures in 3D biological gels affect cell proliferation. Tissue Eng Part A **14,** 379, 2008.
11. Pelham, R.J., Jr., and Wang, Y. Cell locomotion and focal adhesions are regulated by substrate flexibility. Proc Natl Acad Sci U S A **94,** 13661, 1997.
12. Peyton, S.R., Raub, C.B., Keschrumrus, V.P., and Putnam, A.J. The use of poly(ethylene glycol) hydrogels to investigate the impact of ECM chemistry and mechanics on smooth muscle cells. Biomaterials **27,** 4881, 2006.
13. Discher, D.E., Mooney, D.J., and Zandstra, P.W. Growth factors, matrices, and forces combine and control stem cells. Science **324,** 1673, 2009.
14. Reilly, G.C., and Engler, A.J. Intrinsic extracellular matrix properties regulate stem cell differentiation. J Biomech **43,** 55, 2009.
15. Butcher, D.T., Alliston, T., and Weaver, V.M. A tense situation: forcing tumour progression. Nat Rev Cancer **9,** 108, 2009.
16. Gumbiner, B.M. Cell adhesion: the molecular basis of tissue architecture and morphogenesis. Cell **84,** 345, 1996.
17. Nelson, C.M., and Bissell, M.J. Of extracellular matrix, scaffolds, and signaling: tissue architecture regulates development, homeostasis, and cancer. Annu Rev Cell Dev Biol **22,** 287, 2006.
18. Raines, E.W. The extracellular matrix can regulate vascular cell migration, proliferation, and survival: relationships to vascular disease. Int J Exp Pathol **81,** 173, 2000.
19. Discher, D.E., Janmey, P., and Wang, Y.L. Tissue cells feel and respond to the stiffness of their substrate. Science **310,** 1139, 2005.
20. Gray, D.S., Tien, J., and Chen, C.S. Repositioning of cells by mechanotaxis on surfaces with micropatterned Young's modulus. J Biomed Mater Res A **66,** 605, 2003.
21. Ghosh, K., Pan, Z., Guan, E., Ge, S., Liu, Y., Nakamura, T., Ren, X.D., Rafailovich, M., and Clark, R.A. Cell adaptation to a physiologically relevant ECM mimic with different viscoelastic properties. Biomaterials **28,** 671, 2007.
22. Burlew, B.S., and Weber, K.T. Cardiac fibrosis as a cause of diastolic dysfunction. Herz **27,** 92, 2002.
23. Levental, K.R., Yu, H., Kass, L., Lakins, J.N., Egeblad, M., Erler, J.T., Fong, S.F., Csiszar, K., Giaccia, A., Weninger, W., Yamauchi, M., Gasser, D.L., and Weaver, V.M. Matrix crosslinking forces tumor progression by enhancing integrin signaling. Cell **139,** 891, 2009.
24. Le Bousse-Kerdiles, M.C., Martyre, M.C., and Samson, M. Cellular and molecular mechanisms underlying bone marrow and liver fibrosis: a review. Eur Cytokine Netw **19,** 69, 2008.
25. Aneja, A., Tang, W.H., Bansilal, S., Garcia, M.J., and Farkouh, M.E. Diabetic cardiomyopathy: insights into pathogenesis, diagnostic challenges, and therapeutic options. Am J Med **121,** 748, 2008.
26. De Wever, O., Demetter, P., Mareel, M., and Bracke, M. Stromal myofibroblasts are drivers of invasive cancer growth. Int J Cancer **123,** 2229, 2008.
27. Iyengar, P., Espina, V., Williams, T.W., Lin, Y., Berry, D., Jelicks, L.A., Lee, H., Temple, K., Graves, R., Pollard, J., Chopra, N., Russell, R.G., Sasisekharan, R., Trock, B.J., Lippman, M., Calvert, V.S., Petricoin, E.F., 3rd, Liotta, L., Dadachova, E., Pestell, R.G., Lisanti, M.P., Bonaldo, P., and Scherer, P.E. Adipocyte-derived collagen VI affects early mammary tumor progression *in vivo*, demonstrating a critical interaction in the tumor/stroma microenvironment. J Clin Invest **115,** 1163, 2005.
28. Paz, Z., and Shoenfeld, Y. Antifibrosis: to reverse the irreversible. Clin Rev Allergy Immunol **38,** 276, 2009.
29. Sun, Y., Zhang, J.Q., Zhang, J., and Lamparter, S. Cardiac remodeling by fibrous tissue after infarction in rats. J Lab Clin Med **135,** 316, 2000.
30. Sun, Y., and Weber, K.T. Infarct scar: a dynamic tissue. Cardiovasc Res **46,** 250, 2000.
31. Bryant, J.E., Shamhart, P.E., Luther, D.J., Olson, E.R., Koshy, J.C., Costic, D.J., Mohile, M.V., Dockry, M., Doane, K.J., and Meszaros, J.G. Cardiac myofibroblast differentiation is attenuated by alpha(3) integrin blockade: potential role in post-MI remodeling. J Mol Cell Cardiol **46,** 186, 2009.

32. Berry, M.F., Engler, A.J., Woo, Y.J., Pirolli, T.J., Bish, L.T., Jayasankar, V., Morine, K.J., Gardner, T.J., Discher, D.E., and Sweeney, H.L. Mesenchymal stem cell injection after myocardial infarction improves myocardial compliance. Am J Physiol Heart Circ Physiol **290,** H2196, 2006.
33. Breitbach, M., Bostani, T., Roell, W., Xia, Y., Dewald, O., Nygren, J.M., Fries, J.W., Tiemann, K., Bohlen, H., Hescheler, J., Welz, A., Bloch, W., Jacobsen, S.E., and Fleischmann, B.K. Potential risks of bone marrow cell transplantation into infarcted hearts. Blood **110,** 1362, 2007.
34. Hinz, B. Formation and function of the myofibroblast during tissue repair. J Invest Dermatol **127,** 526, 2007.
35. Thakar, R.G., Chown, M.G., Patel, A., Peng, L., Kumar, S., and Desai, T.A. Contractility-dependent modulation of cell proliferation and adhesion by microscale topographical cues. Small **4,** 1416, 2008.
36. Collins, J.M., Ayala, P., Desai, T.A., and Russell, B. Three-Dimensional culture with stiff microstructures increases proliferation and slows osteogenic differentiation of human mesenchymal stem cells. Small **6,** 355, 2009.
37. Bouffard, N.A., Cutroneo, K.R., Badger, G.J., White, S.L., Buttolph, T.R., Ehrlich, H.P., Stevens-Tuttle, D., and Langevin, H.M. Tissue stretch decreases soluble TGF-beta1 and type-1 procollagen in mouse subcutaneous connective tissue: evidence from *ex vivo* and *in vivo* models. J Cell Physiol **214,** 389, 2008.
38. Langevin, H.M., Bouffard, N.A., Badger, G.J., Iatridis, J.C., and Howe, A.K. Dynamic fibroblast cytoskeletal response to subcutaneous tissue stretch *ex vivo* and *in vivo*. Am J Physiol Cell Physiol **288,** C747, 2005.
39. Poobalarahi, F., Baicu, C.F., and Bradshaw, A.D. Cardiac myofibroblasts differentiated in 3D culture exhibit distinct changes in collagen I production, processing, and matrix deposition. Am J Physiol Heart Circ Physiol **291,** H2924, 2006.
40. Wang, J., Seth, A., and McCulloch, C.A. Force regulates smooth muscle actin in cardiac fibroblasts. Am J Physiol Heart Circ Physiol **279,** H2776, 2000.
41. Brown, R.D., Ambler, S.K., Mitchell, M.D., and Long, C.S. The cardiac fibroblast: therapeutic target in myocardial remodeling and failure. Annu Rev Pharmacol Toxicol **45,** 657, 2005.
42. Kleinman, H.K., McGarvey, M.L., Hassell, J.R., Star, V.L., Cannon, F.B., Laurie, G.W., and Martin, G.R. Basement membrane complexes with biological activity. Biochemistry **25,** 312, 1986.
43. Kleinman, H.K., McGarvey, M.L., Liotta, L.A., Robey, P.G., Tryggvason, K., and Martin, G.R. Isolation and characterization of type IV procollagen, laminin, and heparan sulfate proteoglycan from the EHS sarcoma. Biochemistry **21,** 6188, 1982.
44. Diramio, J.A., Kisaalita, W.S., Majetich, G.F., and Shimkus, J.M. Poly(ethylene glycol) methacrylate/dimethacrylate hydrogels for controlled release of hydrophobic drugs. Biotechnol Prog **21,** 1281, 2005.
45. Pfister, P.M., Wendlandt, M., Neuenschwander, P., and Suter, U.W. Surface-textured PEG-based hydrogels with adjustable elasticity: synthesis and characterization. Biomaterials **28,** 567, 2007.
46. Boontheekul, T., Hill, E.E., Kong, H.J., and Mooney, D.J. Regulating myoblast phenotype through controlled gel stiffness and degradation. Tissue Eng **13,** 1431, 2007.
47. Costa-Pinto, A.R., Salgado, A.J., Correlo, V.M., Sol, P., Bhattacharya, M., Charbord, P., Reis, R.L., and Neves, N.M. Adhesion, proliferation, and osteogenic differentiation of a mouse mesenchymal stem cell line (BMC9) seeded on novel melt-based chitosan/polyester 3D porous scaffolds. Tissue Eng Part A **14,** 1049, 2008.
48. Duong, H., Wu, B., and Tawil, B. Modulation of 3D fibrin matrix stiffness by intrinsic fibrinogen-thrombin compositions and by extrinsic cellular activity. Tissue Eng Part A **15,** 1865, 2009.
49. Carver, W., Nagpal, M.L., Nachtigal, M., Borg, T.K., and Terracio, L. Collagen expression in mechanically stimulated cardiac fibroblasts. Circ Res **69,** 116, 1991.
50. Caulfield, J.B., and Janicki, J.S. Structure and function of myocardial fibrillar collagen. Technol Health Care **5,** 95, 1997.
51. Bashey, R.I., Martinez-Hernandez, A., and Jimenez, S.A. Isolation, characterization, and localization of cardiac collagen type VI. Associations with other extracellular matrix components. Circ Res **70,** 1006, 1992.
52. Naugle, J.E., Olson, E.R., Zhang, X., Mase, S.E., Pilati, C.F., Maron, M.B., Folkesson, H.G., Horne, W.I., Doane, K.J., and Meszaros, J.G. Type VI collagen induces cardiac myofibroblast differentiation: implications for postinfarction remodeling. Am J Physiol Heart Circ Physiol **290,** H323, 2006.
53. Sherman-Baust, C.A., Weeraratna, A.T., Rangel, L.B., Pizer, E.S., Cho, K.R., Schwartz, D.R., Shock, T., and Morin, P.J. Remodeling of the extracellular matrix through overexpression of collagen VI contributes to cisplatin resistance in ovarian cancer cells. Cancer Cell **3,** 377, 2003.
54. Mollnau, H., Munkel, B., and Schaper, J. Collagen VI in the extracellular matrix of normal and failing human myocardium. Herz **20,** 89, 1995.
55. Borok, Z. Role for alpha3 integrin in EMT and pulmonary fibrosis. J Clin Invest **119,** 7, 2009.

Address correspondence to:
Tejal A. Desai, Ph.D.
Department of Bioengineering and Therapeutic Sciences
203C Byers Hall Box 2520
1700 4th St.
University of California
San Francisco, CA 94158-2330

E-mail: tejal.desai@ucsf.edu

Received: December 18, 2009
Accepted: March 15, 2010
Online Publication Date: April 19, 2010